

ENGINEERING A CORE – SHELL (Ta- DOPED SrTiO₃)@PTC STRUCTURE FOR HIGH FREQUENCY CAPACITOR APPLICATIONS

**A Dissertation Submitted
in Partial Fulfillment of the Requirement for the
Degree of
MASTERS OF SCIENCE
in
Physics**

**by
Jitendra Singh
Roll No. 24/MSCPHY/26
&
Deepesh Kumar
Roll No. 24/MSCPHY/23**

**Under the supervision of
Dr. Deshraj Meena
Assistant Professor
Department of Applied Physics
Delhi Technological University**



**Department of Applied Physics
DELHI TECHNOLOGICAL UNIVERSITY
(Formerly Delhi College of Engineering)
Shahbad Daulatpur, Main Bawana Road, Delhi-42
MAY, 2026**



DELHI TECHNOLOGICAL UNIVERSITY

(Formerly Delhi College of Engineering)

Shahbad Daultapur, Main Bawana Road, Delhi-42

CANDIDATE'S DECLARATION

We, JITENDRA SINGH, Roll No. 24/MSCPHY/26 and DEEPESH KUMAR, Roll No. 24/MSCPHY/23 students of M.Sc. Physics hereby declares that the project Dissertation titled “**Engineering a Core–Shell (Ta-Doped SrTiO₃)@PTC Structure for High Frequency Capacitor Applications**” which is submitted by us to the Department of Applied Physics, Delhi Technological University, Delhi in partial fulfilment of the requirement for the award of the degree of Master of Science is original and not copied from any source without proper citation. This work has not previously been submitted for the award of any Degree of this or any other Institution.

Candidates Signature

Jitendra Singh

Deepesh Kumar

Date: 29/05/2026

This is to certify that the student has incorporated all the corrections suggested by the examiner in the Dissertation Report and that the statement made by the candidate is correct to the best of our knowledge.

Signature of Supervisor

Dr. Deshraj Meena

Assistant Professor

Department of Applied Physics

Date: 29/05/2026



DELHI TECHNOLOGICAL UNIVERSITY
(Formerly Delhi College of Engineering)
Shahbad Daultapur, Main Bawana Road, Delhi-42

CERTIFICATE BY THE SUPERVISOR

I hereby certify that the Project Dissertation titled " **Engineering a Core-Shell (Ta-Doped SrTiO₃)@PTC Structure for High Frequency Capacitor Applications** " which is submitted by JITENDRA SINGH, Roll No. 24/MSCPHY/26 and DEEPESH KUMAR, 24/MSCPHY/23, Department of Applied Physics, Delhi Technological University, Delhi, in partial fulfilment of the requirement for the award of the degree of Master of Science, is a record of the Dissertation work carried out by the students under my supervision. To the best of my knowledge this work has not been submitted in part or full for any Degree or Diploma to this University or elsewhere.

Signature

Dr. Deshraj Meena

Assistant Professor

Department of Applied Physics

Date: 29/05/2026

ACKNOWLEDGEMENT

We would like to express our deepest sincere gratitude to our supervisor, Dr. Deshraj Meena, Assistant Professor, Department of Applied Physics, Delhi Technological University for giving us the opportunity to work under his guidance and for constant inspiration and incessant support throughout the project. We take this opportunity to express our indebtedness to our supervisor for his enthusiastic help, his expertise, brilliant ideas, valuable suggestions, and constant encouragement. We are grateful to acknowledge the constant help and convenience at every step of our project by all the lab members Ms. Shivani Sangwan, Mr. Gagan Sharma, Ms. Mona Devi, Mr. Mohit Kumar, and Ms. Richa, Dept. of Applied Physics, Delhi Technological University. We are also thankful to our families and friends for their love, care, and support who patiently extended all sorts of help for accomplishing this task.

Deepesh Kumar

Jitendra Singh

ABSTRACT

In this study, Ta-doped SrTiO₃ ($SrTi_{0.997}Ta_{0.003}O_3$) (STTO) was synthesized using the solid-state reaction method, and the formation of the phase was confirmed by X-ray diffraction (XRD) and Fourier transform infrared (FTIR) spectroscopy. The synthesized STTO exhibited a pure cubic perovskite phase with an average crystallite size of ~ 64 nm. An effective approach via core-shell preparation was adopted to suppress grain growth during sintering by utilizing a titanium precursor solution known as Peroxo Titanium Complex (PTC). The PTC solution was employed to form an ultra-thin amorphous shell layer on the nanoparticles, resulting in a core-shell structure in which the STTO nanoparticles act as the core and the PTC layer serves as the shell. The formation of this core-shell structure was confirmed by Transmission electron microscopy (TEM). Further, the dielectric properties of the synthesized core-shell structure were measured within the frequency range 100 Hz to 2 MHz at room temperature. The prepared core-shell structure demonstrated an excellent stability of the dielectric constant and exhibited very low dielectric loss (0.02 to 0.2 for 100 Hz to 2 MHz). Owing to its low dielectric loss at high frequencies, the synthesized material shows strong potential for microwave and other high-frequency capacitor applications.

INDEX

CANDIDATE’S DECLARATION.....	i
CERTIFICATE BY THE SUPERVISOR.....	ii
ACKNOWLEDGEMENT.....	iii
ABSTRACT.....	iv
INDEX.....	v
LIST OF SYMBOLS AND ABBREVIATIONS.....	vii
LIST OF FIGURES.....	viii
CHAPTER 1.....	1
INTRODUCTION.....	1
CHAPTER 2.....	4
LITERATURE REVIEW.....	4
2.1 Overview: Strontium titanate (SrTiO ₃).....	4
2.2 Ta Doping in SrTiO ₃	4
2.3 Core–Shell structure for Dielectric Optimization.....	5
2.4 Research Gap and Motivation for STTO@PTC Core–Shell Design.....	6
CHAPTER 3.....	7
EXPERIMENTAL.....	7
3.1 Material and Reagents.....	7
3.2 Synthesis Methods.....	8
3.2.1 synthesis of SrTi _{0.997} Ta _{0.003} O ₃ ceramics nanoparticles.....	8
3.2.2 Synthesis of PTC (peroxo titanium complex) Shell.....	8
3.2.3 Synthesis of Core-shell structured (SrTi _{0.997} Ta _{0.003} O ₃ @ PTC) nanoparticles.....	9
3.3 Sintering.....	10

CHAPTER 4.....	11
CHARACTERIZATIONS.....	11
4.1 Characterization Techniques.....	11
4.2 Result and discussion.....	11
4.2.1 X- Ray Diffraction (XRD):.....	11
4.2.2 Fourier Transform Infrared Spectroscopy (FTIR):.....	15
4.2.3 TEM analysis:.....	16
4.2.4 Dielectric studies :.....	17
CHAPTER 5.....	21
CONCLUSION	21
References.....	23

LIST OF SYMBOLS AND ABBREVIATIONS

STO	SrTiO ₃
STTO	Ta Doped SrTiO ₃ (SrTi _{0.997} Ta _{0.003} O ₃)
DI water	Deionised water
EPDD	Electron pinned defect dipole
PTC	Peroxo Titanium Complex
CP	colossal permittivity
tanδ	Loss Tangent
XRD	X-ray Diffraction
FTIR	Fourier Transform Infrared Spectroscopy
TEM	Transmission Electron Microscope

LIST OF FIGURES

Figure Name	Page. No.
Fig.1 Schematic representation for the synthesis of (x=0.3wt%)(STTO)	8
Fig. 2 Schematic representation for the synthesis of PTC (peroxo titanium complex)	9
Fig. 3 Schematic representation for the synthesis of core-shell structured STTO@PTC nanoparticles	10
Fig. 4 XRD of Ta Doped SrTiO ₃ with 3wt% Ta Doping	12
Fig.5 XRD patterns of the synthesized (a) STTO nanoparticles, (b) calcined core-shell STTO@PTC powder (3wt%), (c) calcined core-shell STTO@PTC powder (5wt%)	12
Fig. 6 W-H Plot using X- Ray Diffraction (XRD) Data	14
Fig. 7 Fourier Transform Infrared (FTIR) Spectroscopy of the base $SrTi_{1-x}Ta_xO_3$ (x=0.3%) STTO powder	15
Fig. 8 (a) The illustrative representation of core-shell structure , (b-d) TEM images of STTO@PTC Core-shell structure at different scale of magnifications	16
Fig. 9 (a) Deviation in the dielectric constant (K) with the frequency for STTO (0.3 wt%) , STTO@PTC (3 wt%) and STTO@PTC (5 wt%) , sintered at 1200°C , and (b) dielectric loss (tanδ) vs. frequency for STTO(0.3 wt%) , STTO@PTC(3 wt%) , STTO@PTC(5 wt%).	19

CHAPTER 1

INTRODUCTION

Nowadays, researchers are paying increased attention to advanced energy storage technologies due to the rapid dwindling of conventional fossil fuels and their associated environmental impacts [1]. Furthermore, the escalating demand for versatile, highly miniaturized components in microelectronics and modern pulsed-power devices like medical defibrillators, radar has sparked immense interest in eco-friendly, lead-free ceramics exhibiting colossal permittivity (CP)[2]. While traditional ceramic systems such as $BaTiO_3$, $Na_{0.5}Bi_{0.5}TiO_3$, and $CaCu_3Ti_4O_{12}$ (CCTO) often display inspiring CP values, they frequently struggle with severe property variations across different frequencies and operating temperatures [3]. These inherent fluctuations with high dielectric loss, severely limit their real-world device potential. That's why the advancement of lead-free ceramics that can sustain high permittivity ($>10^4$) with minimal dielectric loss ($\tan \delta < 0.1$). And high temperature reliability holds critical value for next-generation energy storage applications [4].

Strontium titanate ($SrTiO_3$) is a prominent candidate that has been extensively explored due to its intrinsically low dielectric loss, amplified breakdown strength, and excellent high-temperature stability. A pure $SrTiO_3$ retain a relatively low intrinsic dielectric permittivity which used to be increased to meet advanced application requirements. Different types of theoretical models have been proposed to explain the origins of induced colossal permittivity in modified titanates. Mainly including the internal barrier layer capacitance (IBLC) effect, electron-pinned defect dipoles (EPDD), and surface barrier layer capacitance (SBLC) [5]. The co-existence of these mechanisms shows a significant challenge in selecting the optimal pathway for material modification. Therefore, developing an effective approach to consistently enhance the dielectric properties of $SrTiO_3$ Ceramics provide ample practical benefits [6].

Defect engineering that is used to provide a highly controlled approach to introducing specific point defects ranks among the most efficient methods for modifying dielectric behavior [7]. A leading technique involves slipping site-occupying point defects into the crystal lattice via acceptor and donor ion doping [8, 9]. In this study, tantalum (Ta^{5+}) is employed as an aliovalent donor dopant to modify the $SrTiO_3$ lattice site. A strategy specifically designed to secure the high-frequency stability and temperature reliability. By Utilizing this defect engineering along with an optimized solid-state reaction process using that Ta-doped $SrTiO_3$ (STTO) ($SrTi_{0.997}Ta_{0.003}O_3$) ceramics were prepared particular targeting the stoichiometric formulation of $SrTi_{0.997}Ta_{0.003}O_3$.

The Ta doped $SrTiO_3$ is widely appreciated for its excellent room-temperature dielectric properties that attain high permittivity along with a strictly maintained low $\tan\delta$. Due to its vigorous permittivity and the environmental advantages of being a lead-free material the STTO is highly preferred for the integration of multilayer ceramic capacitors (MLCCs) [10]. To maintain production, scalability and reliability throughout the growing demand for MLCCs with higher capacitance and smaller footprints. The primary challenge lies in advance optimizing its dielectric performance. Previous studies indicate that the overall dielectric constant and breakdown strength can be enhanced by reducing the grain size to a critical threshold. Thereby limiting long-range leakage currents and domain wall movement [11]. Thus, it is mandatory to evolve methods that effectively control grain growth during sintering without compromising the macroscopic dielectric properties [12].

While modern efforts have employed various sintering additives to tackle these issues. The core-shell architectures have emerged as a far superior solution to evenly distribute these additives at the nanoscale. This overcomes the inhomogeneity problems inherent to traditional ball-milling methods. Coating a thin shell around the highly polarizable STTO core ensures a homogenous spread of secondary phases which boosts densification and tightly controls grain

growth during the sintering process. If conventional low-permittivity materials (such as SiO_2 , TiO_2 or MgO) are used as the shell then they can drastically suppress the overall macroscopic performance of the composite in spite of their microstructural gains [13, 14, 15]. To enhance the dielectric properties while strictly constraining grain growth, this study employs a super-thin TiO_2 shell applied via a peroxo titanium complex (PTC) precursor.

This study focuses on engineering a core-shell Ta-doped $SrTiO_3@PTC$ structure tailored explicitly for high-frequency capacitor applications. In this core-shell Structural design, the Ta-doped $SrTiO_3$ acts as a core and PTC-derived boundary layer functions as an internal capacitive barrier. By physically isolating the highly polarizable STTO grains, this insulating shell effectively disrupts macroscopic leakage current pathways and mitigates detrimental interfacial polarization. This research investigates the microstructural evolution and dielectric mechanics of the STTO@PTC system and aims to demonstrate that precise core-shell encapsulation can suppress high-frequency dielectric loss. Also presenting a robust dielectric constant thereby delivering a highly optimized lead-free dielectric for next-generation pulsed-power and energy storage devices.

CHAPTER 2

LITERATURE REVIEW

2.1 Overview: Strontium titanate (SrTiO₃)

Strontium titanate (SrTiO₃) is a perovskite-structured material. It has gained attention due to its advantageous stable dielectric properties, electronic tunability, and chemical stability [16, 17]. SrTiO₃ plays a vital role in fuel cells by enhancing ionic conduction and improving the stability of electrodes [18]. It also serves as a promising material in different types of supercapacitors, utilizing its large surface area and charge storage capabilities to boost the energy density and improve capacitance [19]. The structure of strontium titanate shows a perovskite ABO₃ structure, with TiO₆ octahedra surrounded by strontium atoms. It used to exhibit a cubic structure above 105 K and transitioned to a different structure below this temperature. Doping in SrTiO₃ with cations of higher oxidation states enhances conductivity by generating electrons and vacancies, which helps to maintain charge balance in the perovskite structure and this results used in improving both electronic and ionic properties [20, 21, 22]. These features of SrTiO₃ make it suitable core material for synthesizing dielectric composites such as core-shell structure.

2.2 Ta Doping in SrTiO₃

Pure SrTiO₃ is a quantum Paraelectric material with a high dielectric constant which increases at low temperatures. Its dielectric permittivity at room temperature remains stable, and dielectric loss can increase under frequency or temperature fluctuations [23, 24]. To overcome these limitations, doping strategies have been widely investigated. Among all the donor dopants, tantalum (Ta⁵⁺) stands out due to its ability to substitute Ti⁴⁺ sites within the lattice. Because the ionic radius of Ta⁵⁺ is slightly larger than that of Ti⁴⁺ that causes measurable lattice expansion and shifting XRD peaks to lower angles, confirming successful doping [19]. This substitution of tantalum introduces positively charged donor states and triggers the formation of

defect dipole clusters, such as $Ti' - V_{O..} - Ti'$ and $Ta. - V_{O..} - 3Ti'$, which enhance local polarization and significantly improve dielectric performance [25, 26]. STTO (Ta doped SrTiO₃) ceramics have been reported to exhibit colossal permittivity ($\epsilon_r \approx 11,423$ at 1 kHz) and remarkably low dielectric loss, which are referred to electron-pinned defect dipole (EPDD) effect mechanisms and controlled oxygen-vacancy complexes [25, 26].

In spite of these remarkable properties, STTO still suffers from many issues such as leakage currents, microstructural inhomogeneity, and grain-boundary conduction losses at higher frequencies. These limitations necessitate additional structural control, where core-shell engineering becomes a highly effective approach.

2.3 Core-Shell structure for Dielectric Optimization

Core-shell structures have gained prominence for tailoring electrical responses in dielectric materials by containing a high-permittivity core with an insulating or semi-insulating shell. It is used to simultaneously accomplish :

- Improved interfacial polarization
- Enhance thermal stability
- Depletion of dielectric loss
- Management of microstructural heterogeneity

For SrTiO₃-based dielectrics, the core-shell abstract idea allows the high intrinsic permittivity of the core to be retained while engineering an insulating shell that limits conduction losses [27]. This structure also raises a Maxwell-Wagner interfacial polarization effect, which can further upgrade effective permittivity.

Peroxo Titanium Complex (PTC) Material shows strong resistivity modulation due to grain-boundary barrier layers when it used as a shell substance around high-k SrTiO₃ particles it serve multiple beneficial functions [15] :

- They make a resistive boundary layer that blocks charge jumping and leakage currents, effectively reducing dielectric loss.
- Thermal stability is enhanced as PTC materials naturally exhibit temperature-driven resistance increases, stabilizing dielectric behaviour.

2.4 Research Gap and Motivation for Ta doped SrTiO₃@PTC Core–Shell Design

- Grain-boundary conduction can still contributed to the dielectric loss.
- Leakage pathways are affected by the colossal permittivity of the materials.
- Frequency-dependent response requires enhanced control of microstructural heterogeneity.

core–shell engineering Ta doped SrTiO₃@PTC offers better solutions to these challenges but remains underexplored. The combination of Ta-doped SrTiO₃ as the core with a PTC shell acting as a resistive barrier represents a powerful approach for achieving high permittivity as well as low dielectric loss, which is indispensable for next-generation energy storage devices and high-frequency capacitor applications.

CHAPTER 3

EXPERIMENTAL

3.1 Material and Reagents

Raw materials including Strontium Hydroxide Octahydrate ($Sr(OH)_2 \cdot 8H_2O$ – 99.96 % purity), Titanium Dioxide (TiO_2 – 99.94% purity), Tantalum Penta-oxide (Ta_2O_5 – 99.99%) purchased from (Sigma Aldrich). Hydrogen Peroxide (H_2O_2 – 99.4%) as Oxidizing agent, Titanium Hydride (TiH_2 – 99.9%), Ammonium Hydroxide (NH_4OH – 99.9%) as base catalyst, 5% PVA as binder and Deionized water (DI) water.

Solid State Synthesis:

Solid state synthesis commonly referred to as the ceramic method chemical process in which a new solid compound having an already known structure is synthesized using solid precursors. The products derived from this process are widely used in the energy and electrical area. These products cover polycrystals, single crystals, glasses and thin-film materials.

The overall concept is that the fine-grain metallic mixture is homogenised pressed to make pellets which then is heated for a particular temperature for a particular time. Some metal compounds for example, metallic oxides in combination with salts require harsh environments like high pressure and temperature for processing either as a melted flux or a rapid condensing vapor phase.

Evaluation of rate of reaction in solid state process is very important because purification methods available to recover these solid products are extremely poor, so the reactions must be carried out until the completion. The rate of reaction in solid state synthesis is dependent on lots of factors such as structure factors, arrangement and rate of diffusion and thermodynamics concerning reactions.

3.2 Synthesis Methods

3.2.1 synthesis of $SrTi_{1-x}Ta_xO_3$ (x=0.3wt%) nanoparticles

$SrTi_{1-x}Ta_xO_3$ (x=0.3wt%) has been prepared using the solid-state reaction method, abbreviated as STTO. Based on the pretended stoichiometric ratio of the target compound, the raw materials such as $Sr(OH)_2 \cdot 8H_2O$, TiO_2 and Ta_2O_5 were accurately weighted. The mixture was grinded in the mortar and pestle with the help of DI water for 12 hours to achieve uniform mixing. After completing the initial hand grinding, the resulting powder was dried and calcined at 1150°C for 2 hours. The calcined powder underwent another 12 hour hand grinding and followed by drying. Thus, we obtained $SrTi_{1-x}Ta_xO_3$ (x=0.3wt%) nanoparticles, a schematic diagram have been shown in Fig.1.

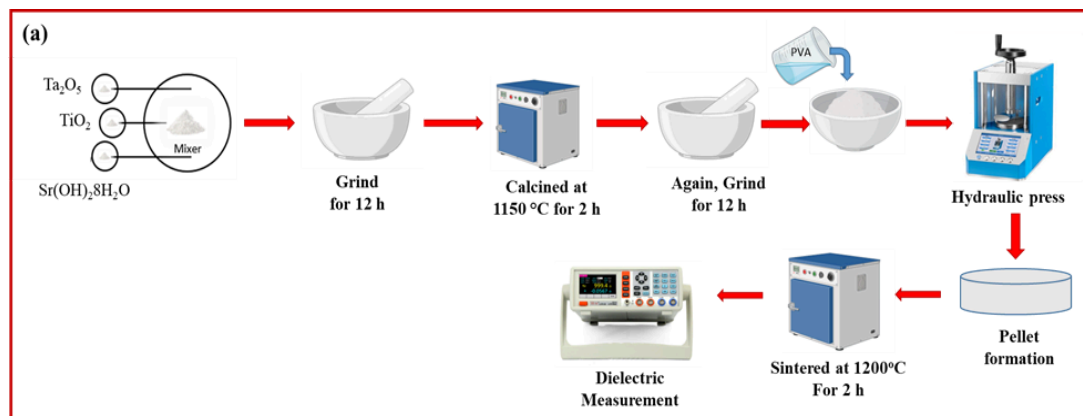


Fig. 1 Schematic representation for the synthesis of $SrTi_{1-x}Ta_xO_3$ (x=0.3wt%) (STTO)

3.2.2 Synthesis of PTC (peroxo titanium complex) Shell

To prepare the PTC solution for the shell layer, as shown in Fig. 2, 10 ml of H_2O_2 (oxidizer) kept on stirring for 40 minutes in a jacketed beaker at 50°C temperature. During this process 25 mg of TiH_2 and a little drop of NH_4OH (base catalyst) was added to the solution. The resulted solution was again stirred in a jacketed beaker,

keeping the temperature below 50°C for 1h. Once the TiH_2 dissolved fully, a yellowish transparent solution was obtained, this was the PTC solution.

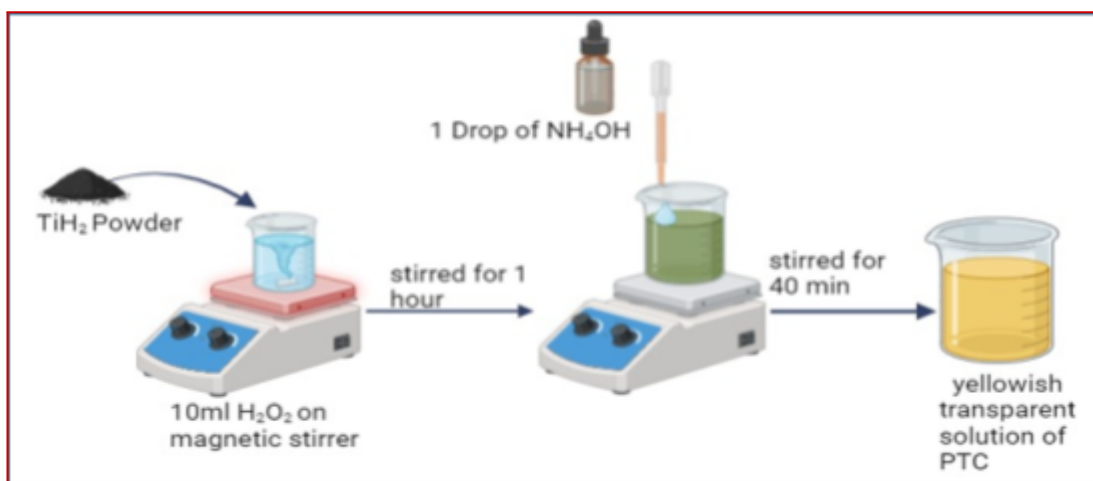


Fig. 2 Schematic representation for the synthesis of PTC (peroxo titanium complex)

3.2.3 Synthesis of Core-shell structured ($SrTi_{1-x}Ta_xO_3 @ PTC$) nanoparticles

For the coating of PTC shell on the surface of $SrTi_{1-x}Ta_xO_3$ (STTO), STTO powder was added to the deionized water (DI) and mixed by the bath ultrasonicator. Then the PTC solution was dropwise added to $SrTi_{1-x}Ta_xO_3$ (STTO) suspension and stirred at 350 rpm at 70°C for 12 hours. To investigate the microstructure and dielectric properties, PTC amount has been varied (3 and 5wt%) which will help to compare microstructure and dielectric trends of the nanoparticles. After completing the reaction, the dissolved STTO@PTC suspension was centrifuged and the precipitate has been collected to at 80°C for 12 hours. After the natural cooling, we obtained core-shell structured (STTO@ PTC) nanoparticles.

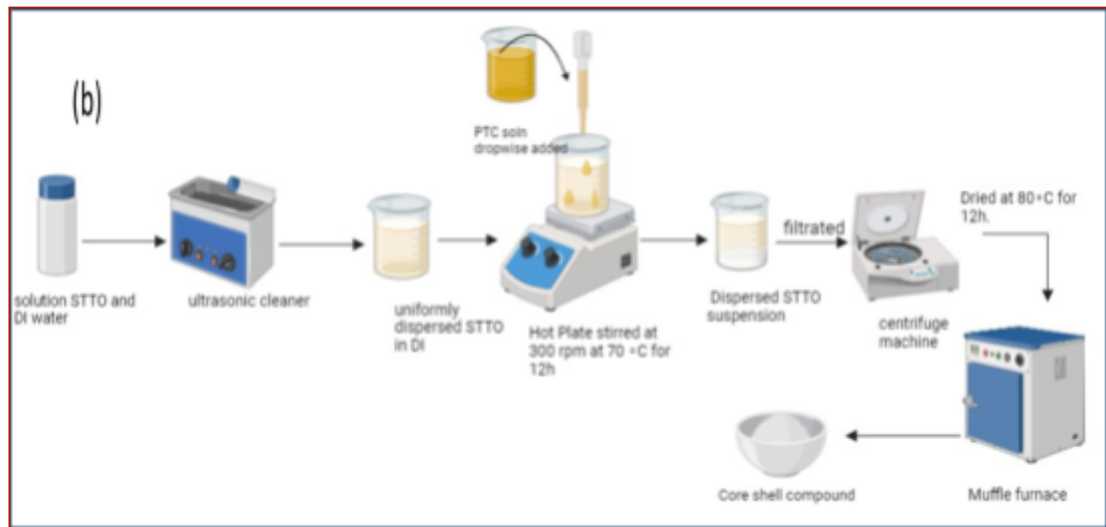


Fig.3 Schematic representation for the synthesis of core-shell structured STTO@PTC nanoparticles

3.3 Sintering

The fabricated PTC - coated STTO core -shell particles were compacted into pellets using uniaxial pressing via hydraulic press. The pellets of diameter 6 mm and a thickness of 1mm have been prepared under a pressure of 20 MPa. To improve the mechanical strength of a pellet, the organic PVA binder was used. The resulting pellets were then isothermally sintered at temperatures 1150°C and 1200°C for 2 hours, with a heating rate of 5°C per minute.

CHAPTER 4

CHARACTERIZATIONS

4.1 Characterization Techniques

To confirm the crystal structure of synthesized samples, Bruker D8 Discover X – ray diffractometer with X – ray source of Cu K (1.54 Å) has been used. Perkin Elmer used to carry out Fourier Transform Infrared Spectroscopy (FTIR) which successfully identified the functional group and chemical bonding within Ta Doped SrTiO₃. Technai G2 T30, U-Twin Transmission Electron Microscope (TEM) was used to confirm the coating of PTC layer on STTO. Further, dielectric properties have been studied within a wide frequency (100Hz -2MHz) range at room temperature using a Hioki LCR meter (Model IM3536) and a PID temperature controller (Model 234).

4.2 Result and discussion

4.2.1 X- Ray Diffraction (XRD):

A non-destructive technique that analyses the atomic and molecular structure of a crystal and the crystallite size, phase and internal stress within micro crystalline regions is called X-ray crystallography.

Fig. 5 represents the XRD pattern of the synthesized Ta-doped SrTiO₃ and the core-shell structure STTO@PTC. The observed diffraction peaks of STTO (Fig. 5(a)) have been observed 22.8°, 32.22°, 40.0°, 46.30°, 52.5°, 57.63°, 68.6°, 72.5° and 78.° that correspond to (100), (110), (111), (200), (210), (211), (220), (221), and (310) planes and has been matched with JCPDS file No. 35-0734. It is found that all samples show a pure cubic perovskite phase with space group Pm-3m [28, 29]. The observed result shows that during the synthesis of STTO, the Ta ions have been successfully consolidated into the crystal lattice of SrTiO₃, producing a slight shift in (110) diffraction peak [29]. Fig. 5(b) and 5(c) show the XRD patterns of the calcined STTO@PTC core-shell structure with 3wt% and 5wt% of PTC, respectively.

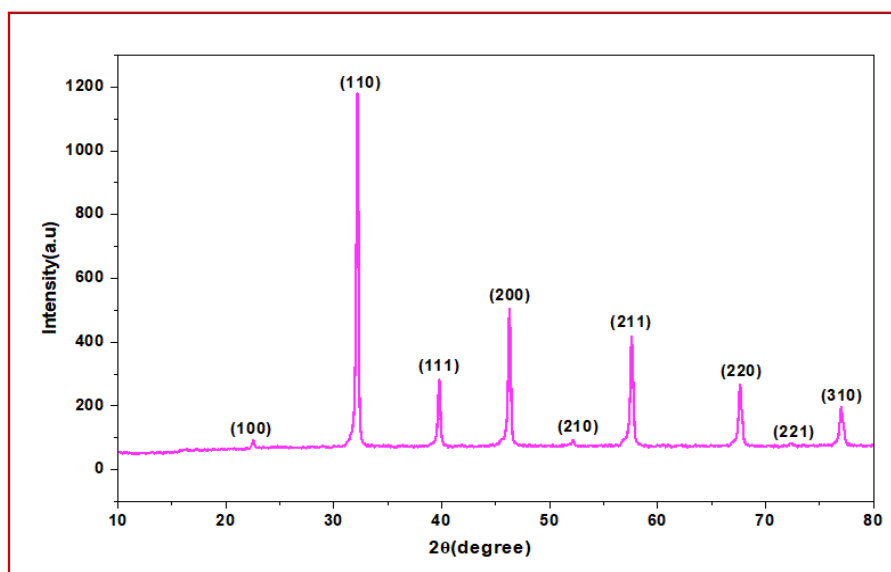


Fig. 4 XRD of Ta Doped SrTiO₃ with 3wt% Ta Doping.

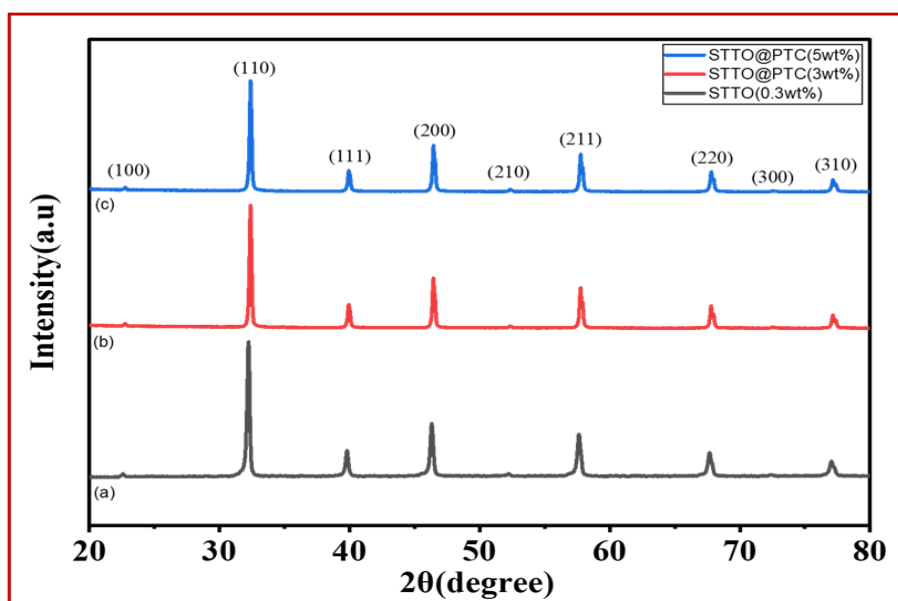


Fig. 5 XRD patterns of the synthesized (a) STTO nanoparticles, (b) calcine core-shell STTO@PTC powder (3wt%), (c) calcined core-shell STTO@PTC powder (5wt%)

The diffraction patterns closely match with the crystalline $SrTiO_3$ and no secondary phases have been detected [30]. Concurrently, the absence of macroscopic crystalline TiO_2 reflections suggests that the peroxo titanium complex (PTC) precursor may have formed an amorphous or finely dispersed nanoscale boundary layer at the STTO particles interfaces as there are no specific crystalline peaks for TiO_2 in XRD patterns of STTO@PTC [31].

There is a small shift in (110) diffraction peak. This peak shift leads to the larger ionic radius of Ta^{5+} compared to Ti^{4+} . Due to the substitution of Ta^{5+} in the place of Ti^{4+} interplaner increases and this results in an increase in the volume of the unit cell.

To calculate the crystallite size of synthesized material Scherrer's formula was used, the formula given as

$$D = \frac{K\lambda}{\beta \cos\theta} \quad (1)$$

Where,

D = Crystallite Size

K= Shape factor = 0.9

λ = Wavelength of CuK_α (1.54 Å)

β = FWHM

θ = Bragg's angle

The average crystallite size was found 63 nm. This size of crystallites represent that very fine nanoparticles were created. Further for calculating microstrain present in the nanoparticles 'Uniform Deformation Method' was used and with the help of the Willum -Hall plot which is given in figure.5 microstrain successfully calculated. The following Scherrer equation with strain given as

$$\beta_{total} = \frac{K\lambda}{D\cos\theta} + 4\epsilon\tan\theta \quad (2)$$

Or

$$\beta\cos\theta = 4\epsilon\sin\theta + \frac{K\lambda}{D} \quad (3)$$

where, β is the Full width at half maximum, θ is the Bragg's angle and ϵ is the slope of the W-H plot where it represents the microstrain present in the nanoparticles. $\frac{K\lambda}{D}$ is the intercept in the W-H plot which is used to calculate crystallite size.

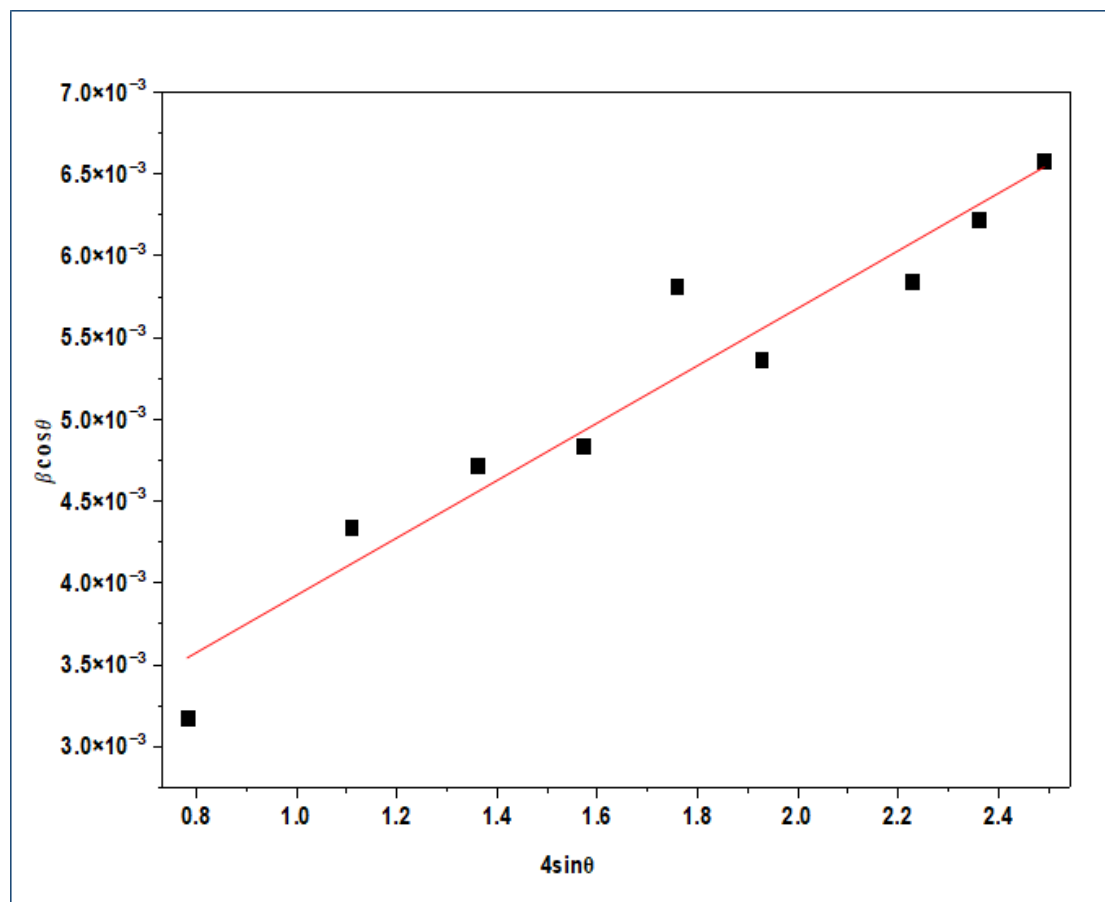


Fig. 6 W-H Plot using X- Ray Diffraction (XRD) Data

4.2.2 Fourier Transform Infrared Spectroscopy (FTIR):

Fourier Transform Infrared (FTIR) spectroscopy was utilized to evaluate the chemical bonding and surface characteristics of the Ta-doped SrTiO₃ (STTO) powder. Fig. 7 represents the FTIR spectra for the synthesized samples. The low-frequency region of the spectrum exhibits robust absorption bands at 525 cm⁻¹, 480 cm⁻¹, and 855 cm⁻¹ which correspond to the characteristic stretching vibration of Sr – Ti – O, bending vibrations of Ti – O, and stretching of Ti – O₆ octahedra, respectively [32]. Because the doping concentration was so incredibly tiny (0.3wt%), and because Ta and Ti have relatively similar atomic properties, the vibration of the Ta – O bond is practically identical to the Ti – O bond [33]. Further, the infrared peak at 1485 cm⁻¹ indicates hydroxyl (-OH) group from the adsorbed water [32]. Because these polar surface species can act as charge trapping centers and facilitate surface ionic conduction that inherently increases dielectric loss under high-frequency alternating electric fields [34].

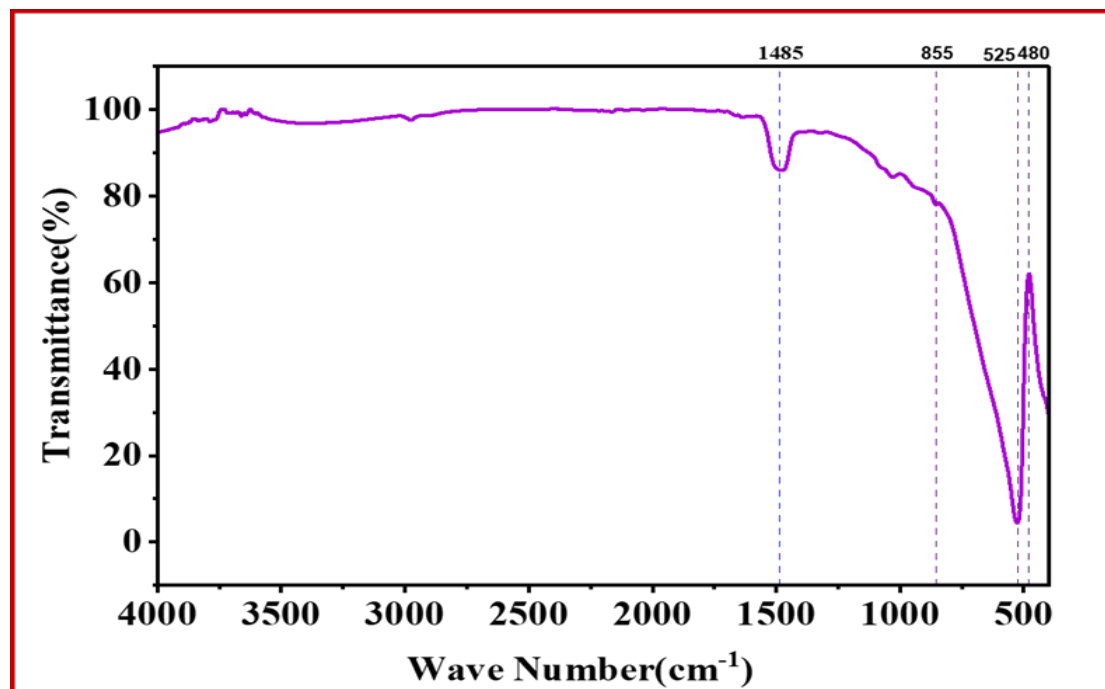


Fig. 7 Fourier Transform Infrared (FTIR) Spectroscopy of the base $SrTi_{1-x}Ta_xO_3$ ($x=0.3\%$) STTO powder

4.2.3 TEM analysis:

Transmission Electron Microscopy (TEM) was employed to visually confirm the morphological evolution and structural encapsulation of the STTO@PTC composites. Fig. 8 shows the illustrative demonstration of the prepared core-shell structured STTO@PTC nanoparticles (Fig. 8(a)) with their morphological features as revealed by TEM images. The highly - magnified TEM images as shown in Fig.8 (b-d), certainly reveals a distinct core-shell structure ,characterized by a dark , electron-concentrate (STTO) core enveloped by a lighter colour i.e., amorphous-like Peroxo Titanium Complex (PTC) derived as TiO_2 shell. The calculated shell thickness is uniformly maintained at approximately 32 nm , clearly defined by the mass-thickness contrast between the crystalline- core and the applied boundary

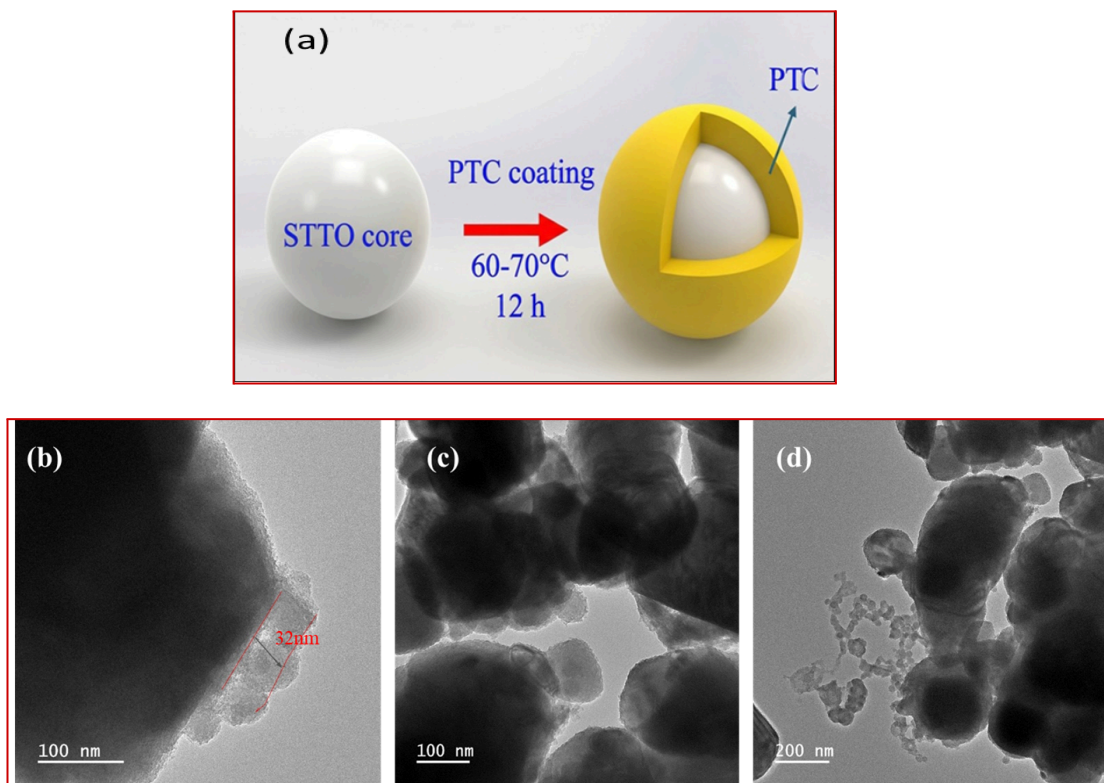


Fig. 8 (a) The illustrative representation of core-shell structure , (b-d) TEM images of STTO@PTC Core-shell structure at different scale of magnifications

coating [35]. These TEM images illustrate that this encapsulating layer successfully covers the individual base (STTO) particles , avoiding direct physical contact

between the highly polarizable STTO cores [36]. From a dielectric engineering point of view, this ~32 nm wide continuous interfacial layer is of key importance for high-frequency capacitor applications.

It behaves as an analytical, structural and electrical barrier that hinders long-range charge carrier transport and interfacial polarization. By physical isolation of STTO grains, the PTC shell successfully disrupts continuous leakage current pathways, thereby suppressing dielectric loss ($\tan(\delta)$) and intensely enhancing the overall breakdown strength of the prepared composite [37].

4.2.4 Dielectric studies :

Fig. 9 shows the frequency dependence of the dielectric constant (K or ϵ') and dielectric loss ($\tan\delta$) for the $SrTi_{1-x}Ta_xO_3$ @ PTC nanoparticles sintered at 1200°C at room temperature across a high-frequency range (100Hz–2000 kHz). As depicted in Fig. 8a, the base STTO core exhibits the highest dielectric constant ($K \approx 160$) that remains remarkably stable across the measured frequency spectrum. Upon encapsulation with the PTC-derived TiO_2 shell, the effective permittivity of the composites drastically decreases. The STTO@PTC (3wt%) sample exhibits a dielectric constant $K \approx 50$ while the 5wt% sample stabilizes near $K \approx 70$ at higher frequencies.

The highly polarizable STTO grain and the insulating TiO_2 boundary layer act as two capacitors in series. This behavior is mathematically described by the classic series mixing model for Internal Barrier Layer Capacitors (IBLC):

$$\frac{1}{C_{total}} = \frac{1}{C_{core}} + \frac{1}{C_{shell}} \quad (4)$$

In terms of effective permittivity (ϵ_{eff}) and volume fractions (V):

$$\epsilon_{eff} = \frac{\epsilon_{core} \epsilon_{shell}}{V_{core} \epsilon_{shell} + V_{shell} \epsilon_{core}} \quad (5)$$

Because the intrinsic permittivity of the amorphous/nanocrystalline TiO_2 shell is lower than that of the Ta-doped SrTiO_3 perovskite core, the low-permittivity shell dominates the denominator. This shell acts as an electrostatic bottleneck that inherently reduces the macroscopic dielectric constant of the bulk material [38].

While the dielectric constant is reduced, the true advantage of the core-shell architecture is revealed in the dielectric loss spectrum (fig. 9b). The dielectric loss or dissipation factor represents the ratio of dissipated electrical energy to stored energy:

$$\tan\delta = \frac{\epsilon''}{\epsilon'} \quad (6)$$

where ϵ'' is the imaginary part of permittivity and ϵ' is the real part of permittivity. Reducing this ratio is the primary objective for high frequency capacitor applications.

The STTO@PTC (3wt %) sample represents an exceptionally low and stable dielectric loss ($\text{TiO}_2 < 0.02$) across the entire 100Hz–2000 kHz range. This confirms that the shell layer generated at 3wt% successfully suppresses long-range leakage currents between STTO grains without introducing excessive defect states. By increasing the PTC shell concentration to 5 wt% induces a degradation in performance that characterized by a massive low-frequency loss spikes ($\text{TiO}_2 > 0.20$) and a sustained at high-frequency plateau ($\text{TiO}_2 \approx 0.05$). This phenomenon is managed by Maxwell-Wagner-Sillars (MWS) interfacial polarization [34]. The variation in thickness of TiO_2 coating leads to an excessive accumulation of space charges at the STTO/ TiO_2 interface. Under an alternating high-frequency electric field. The **relaxation time** (τ) of these trapped charges causes them to oscillate out of phase with the field and dissipating electrical energy as heated according to the Debye relaxation model:

$$\epsilon''_{MWS} \propto \frac{\omega\tau}{1 + \omega^2\tau^2} \quad (7)$$

where ω is the angular frequency.

At 5 wt%, the complete volume of oscillating interfacial charges massively inflates ϵ'' , destroying the low-loss profile required for high-frequency efficiency [39]. Thus,

the frequency-dependent dielectric spectra indicate that the 3 wt% PTC coating provides

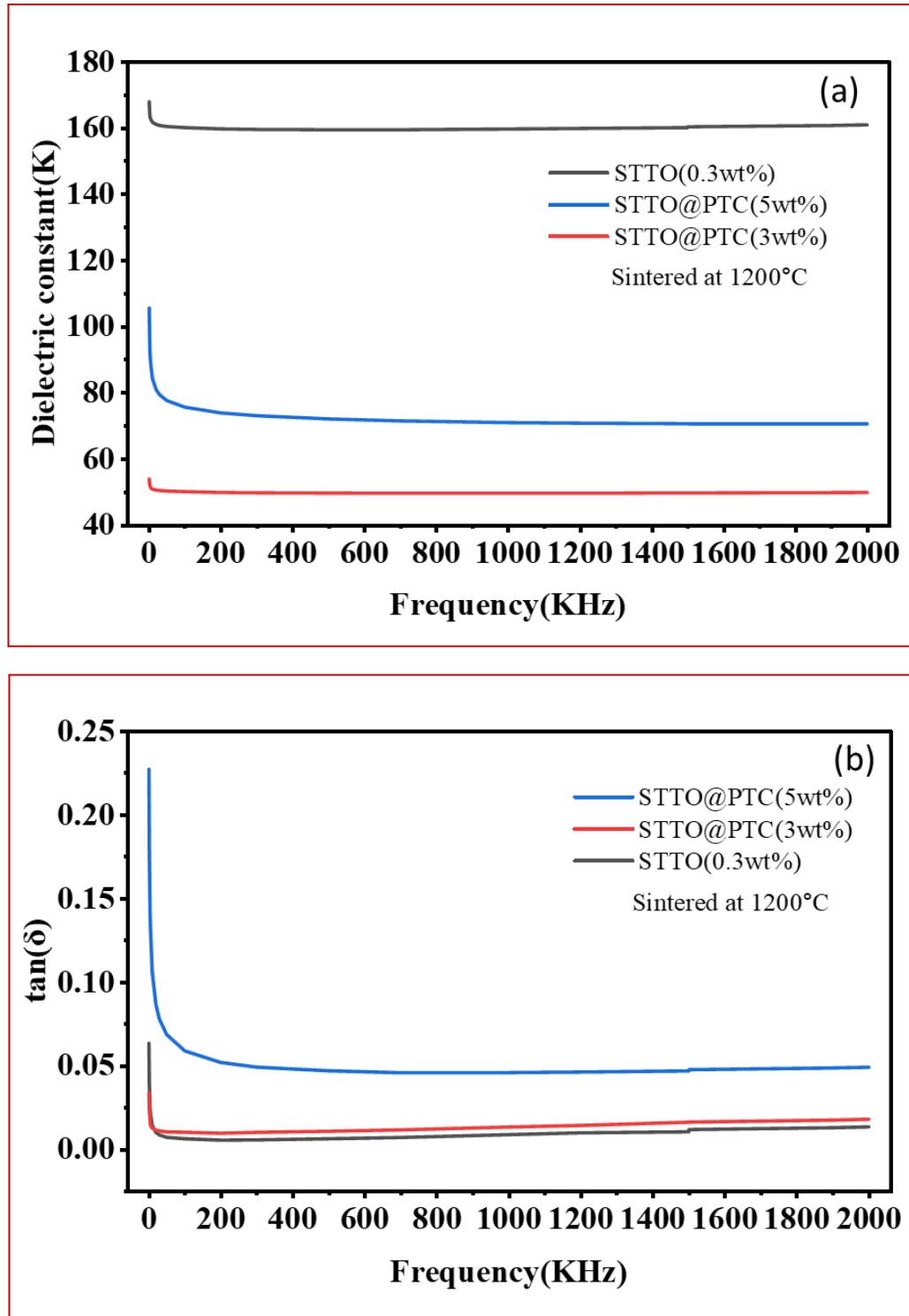


Fig. 9 (a) Deviation in the dielectric constant (K) with the frequency for STTO (0.3 wt%), STTO@PTC (3 wt%) and STTO@PTC (5 wt%), sintered at 1200°C, and (b)

dielectric loss ($\tan\delta$) vs. frequency for STTO(0.3 wt%) , STTO@PTC(3 wt%) , STTO@PTC(5 wt%).

optimal microstructural balance for the STTO core. The insulating TiO_2 shell significantly reduces the macroscopic dielectric constant via the internal series capacitor effect. This specific boundary layer thickness is highly effective at physically disrupting long-range leakage currents. The performance degradation and massive loss spike observed in the 5 wt% sample further underscore that strictly limiting the shell volume fraction is critical to preventing the Maxwell-Wagner-Sillars interfacial polarization. The dielectric data indicates that the STTO@PTC (3wt%) composite successfully achieves a low-loss electrical profile for high-frequency capacitor applications [[35](#), [40](#), [41](#)].

CHAPTER 5

CONCLUSION

In summary, Ta-doped strontium titanate ($SrTi_{0.997}Ta_{0.003}O_3$; STTO) was successfully synthesized through a solid-state reaction method with pure cubic perovskite phase and verified by XRD and FTIR spectroscopy. The synthesis of a core-shell structure (STTO@PTC), validated by TEM analysis, proved to be the definite factor in optimizing dielectric performance. As the impedance spectroscopy brings out that the 0.3wt% Ta-doped $SrTiO_3$ exhibits a dielectric constant of approximately 160. The introduction of a 3wt% PTC shell results in a stable, effective dielectric constant of approximately 50. This 3wt% core-shell configuration gets a remarkable decrease in dielectric loss, maintaining a highly stable dissipation factor of $\tan\delta < 0.02$ over the investigated frequency range (100Hz to 2 MHz). This result shows superior frequency stability compared to the STTO, as the PTC shell helpfully suppresses leakage currents as well as interfacial polarization. On the other hand, experimental data suggested that exceeding this optimal shell concentration (e.g., 5wt% PTC) leads to the performance degradation, characterized by an expressive loss spike ($TiO_2 > 0.20$) at low frequencies. These conclusions emphasize that the core-shell of STTO@PTC structure can be used for high-frequency capacitor applications, offering a highly encouraging material for next-generation, low- $\tan\delta$ electronic components and high-stability energy storage systems.

For future work we will study core-shell structure dielectric properties with varying thickness of PTC coating.

CERTIFICATES





References

1. Yang, L., Kong, X., Li, F., Hao, H., Cheng, Z., Liu, H., Li, J. F., & Zhang, S. (2019). Perovskite lead-free dielectrics for energy storage applications. *Progress in Materials Science*, 102, 72-108. <https://doi.org/10.1016/j.pmatsci.2018.12.005>
2. Pan, H., Li, F., Liu, Y., Zhang, Q., Wang, M., Lan, S., ... & Lin, Y. (2019). Ultrahigh-energy density lead-free dielectric films via polymorphic nanodomain design. *Science*, 365(6453), 578-582. <https://doi.org/10.1126/science.aaw8109>
3. Sinclair, D. C., Adams, T. B., Morrison, F. D., & West, A. R. (2002). CaCu₃Ti₄O₁₂: One-step internal barrier layer capacitor. *Applied Physics Letters*, 80(12), 2153-2155. <https://doi.org/10.1063/1.1463211>
4. Guo, X., Pu, Y., Ji, J., et al. (2020). Colossal permittivity and high insulation resistivity in Dy-modified SrTiO₃ lead-free ceramic materials with low dielectric loss. *Ceramics International*, 46(8), 10075-10082. <https://doi.org/10.1016/j.ceramint.2019.12.275>
5. Hu, W., Liu, Y., Withers, R. L., Frankcombe, T. J. et al. (2013). Electron-pinned defect-dipoles for high-performance colossal permittivity materials. *Nature Materials*, 12(9), 821-826. <https://doi.org/10.1038/nmat3691>
6. Guo, X., Pu, Y., Wang, W., Zhang, et al. (2019). High Insulation Resistivity and Ultralow Dielectric Loss in La-Doped SrTiO₃ Colossal Permittivity Ceramics through Defect Chemistry Optimization. *ACS Sustainable Chemistry & Engineering*, 7(15), 13041-13052. <https://doi.org/10.1021/acssuschemeng.9b02143>
7. Zhao, P., Fang, Z., Zhang, X., Chen, et al. (2021). Aliovalent Doping Engineering for A- and B-Sites with Multiple Regulatory Mechanisms: A Strategy to Improve Energy Storage Properties of Sr_{0.7}Bi_{0.2}TiO₃-Based Lead-Free Relaxor Ferroelectric Ceramics. *ACS Applied Materials & Interfaces*, 13(21), 24833-24855. <https://doi.org/10.1021/acsaami.1c04274>

8. Feng, Y., Wu, J., Chi, Q., Li, W., Yu, Y., & Fei, W. (2020). Defects and Aliovalent Doping Engineering in Electroceramics. *Chemical Reviews*, 120(3), 1710-1787. <https://doi.org/10.1021/acs.chemrev.9b00507>
9. Kovalevsky, A. V., Populoh, S., Patrício, S. G., et al. (2015). Design of SrTiO₃-Based Thermoelectrics by Tungsten Substitution. *The Journal of Physical Chemistry C*, 119(9), 4466-4478. <https://doi.org/10.1021/jp510743h>
10. Zhao, P., Cai, Z., Wu, L., et al. (2021). Perspectives and challenges for lead-free energy-storage multilayer ceramic capacitors. *Journal of Advanced Ceramics*, 10(6), 1153-1193. <https://doi.org/10.1007/s40145-021-0516-8>
11. Gong, H., Wang, X., Zhang, S., et al. (2014). Grain size effect on electrical and reliability characteristics of modified fine-grained BaTiO₃ ceramics for MLCCs. *Journal of the European Ceramic Society*, 34(7), 1733-1739. <https://doi.org/10.1016/j.jeurceramsoc.2013.12.028>
12. Zhang, Y., Zhou, G., Zhang, Y., et al. (2025). Simultaneous Realization of High Dielectric Constant and Ultrahigh Quality Factor in SrTiO₃ via a Tunable Grain Growth Strategy. *ACS Applied Materials & Interfaces*, 17(40). <https://doi.org/10.1021/acsami.5c11750>
13. Fan, Y., Huang, X., Wang, G., & Jiang, P. (2015). Core–Shell Structured Biopolymer@BaTiO₃ Nanoparticles for Biopolymer Nanocomposites with Significantly Enhanced Dielectric Properties and Energy Storage Capability. *The Journal of Physical Chemistry C*, 119(49), 27330-27339. <https://doi.org/10.1021/acs.jpcc.5b09619>
14. Luo, H., Zhang, D., Jiang, C., et al. (2015). Improved Dielectric Properties and Energy Storage Density of Poly(vinylidene fluoride-co-hexafluoropropylene) Nanocomposite with Hydantoin Epoxy Resin Coated BaTiO₃. *ACS Applied Materials & Interfaces*, 7(15), 8061-8069. <https://doi.org/10.1021/acsami.5b00555>
15. D. Lee, H. Kim, C. Kim, et al., Preparation of homogeneous structured core-shell BaTiO₃ particles for high energy storage capacitor

- applications, *Ceramic International* 51 (2025) 37525-37532.
<https://doi.org/10.1016/j.ceramint.2025.06.004>
16. K . S Randhawa, Advanced ceramics in energy storage applications: Batteries to hydrogen energy, *J Energy Storage* 98 (2024) 113122.
<https://doi.org/10.1016/j.est.2024.113122>
17. M.A. Morsi, A.M. Alghamdi, E. Banoqitah, A.E. Tarabiah, et al. Preparation, structural, morphological, optical, electrical, mechanical, and thermal properties of perovskite SrTiO₃ nanoparticles boosted PVA/PEO blend for flexible optoelectronic and capacitor applications, *Ceram. Int.* 50 (18, Part A) (2024) 33027–33039.
<https://dx.doi.org/10.1016/j.ceramint.2024.06.117>
18. G. Chen, H. Liu, Y. He, L. Zhang, M.I. Asghar, S. Geng, P.D. Lund, Electrochemical mechanisms of an advanced low-temperature fuel cell with a SrTiO₃ electrolyte, *J Mater Chem A* 7 (16) (2019) 9638–9645.
<https://doi.org/10.1039/C9TA00499H>
19. K. Karthick, S.R. Ede, U. Nithiyantham, S. Kundu, Low-temperature synthesis of SrTiO₃ nanoassemblies on DNA scaffolds and their applications in dye- sensitized solar cells and supercapacitors, *New J. Chem.* 41 (9) (2017) 3473–3486. <https://doi.org/10.1039/C7NJ00204A>
20. M. Rizwan, A. Ali, Z. Usman, N.R. Khalid, H.B. Jin, C.B. Cao, Structural, electronic and optical properties of copper-doped SrTiO₃ perovskite: A DFT study, *Phys. B Condens. Matter* 552 (2019) 52–57.
<https://doi.org/10.1016/j.physb.2018.09.022>
21. Y. Wang, S. Wang, X. Yu, L. Cao, M. Mao, H.B. Bafroei, Z. Lu, K. Song, D. Wang, Dramatic impact of raw chemicals on the electrical properties of SrTiO₃ ceramics, *Ceram. Int.* 23 (2024) 51841–51847.
<https://doi.org/10.1016/j.ceramint.2024.02.218>
22. J.S. Yoon, M.Y. Yoon, C. Kwak, H.J. Park, S.M. Lee, K.H. Lee, H.J. Hwang, Y_{0.08}Sr_{0.92}Fe_xTi_{1-x}O_{3-δ} perovskite for solid oxide fuel cell anodes, *Mater. Sci. Eng. B* 177 (2) (2012) 151–156.
<https://doi.org/10.1016/j.mseb.2011.10.016>

23. L. Liu, B. Chu, P. Li, et al., Achieving high energy storage performance and ultrafast discharge speed in SrTiO₃-based ceramics via a synergistic effect of chemical modification and defect chemistry, *Chem. Eng. J.* 429 (2022) 132548. <https://doi.org/10.1016/j.cej.2021.132548>
24. W. Bai, Y. Zhou, M. Xiao, et al., Effects of Cu ion implantation on the microstructure, dielectric and impedance properties of SrTiO₃ ceramics prepared by reduction-reoxidation method, *Ceram. Int.* 50 (22) (2024) 46279–46287. <https://doi.org/10.1016/j.ceramint.2024.08.470>
25. W. Pan, M. Cao, H. Hao, et al., Defect engineering toward the structures and dielectric behaviors of (Nb, Zn) co-doped SrTiO₃ ceramics, *J. Eur. Ceram. Soc.* 40 (1) (2020) 49–55. <https://doi.org/10.1016/j.jeurceramsoc.2019.09.027>
26. R. Gu, X. Guo, J. Kang, et al., Colossal permittivity and ultralow dielectric loss in SrTi_{1-x}Nb_xO₃ ceramics sintered at different atmospheres via defect chemistry improvement, *Ceram. Int.* 48 (9) (2022) 12692–12698. <https://doi.org/10.1016/j.ceramint.2022.01.138>
27. D He, Y Wang, et al., Core–shell structured BaTiO₃@Al₂O₃ nanoparticles in polymer composites for dielectric loss suppression and breakdown strength enhancement, *Composite part A: Applied Sci. and Manufacturing* 93 (2017) 137–143. <https://doi.org/10.1016/j.compositesa.2016.11.025>
28. J. Liu, C.L. Wang, Y. Li, W.B. Su, Y.H. Zhu, J.C. Li, L.M. Mei, Influence of rare earth doping on thermoelectric properties of SrTiO₃ ceramics, *J. Appl. Phys.* 114 (2013), <https://doi.org/10.1063/1.4847455>.
29. Keying Xue, Lingxia Li, ‘Colossal permittivity in Ta-doped SrTiO₃ ceramics induced by interface effects and defect structure: An experimental and theoretical study’ *Ceramics International* 49(2023) 20388–20397, <https://doi.org/10.1016/j.ceramint.2023.03.167>
30. Shen, Z., Wang, X., Luo, B., & Li, L. (2015). BaTiO₃–BiYbO₃ perovskite materials for energy storage applications. *Journal of Materials Chemistry A*, 3(35), 18146–18153. <https://doi.org/10.1039/C5TA03614C>

31. Li, W., et al. (2018). Core-shell structured BaTiO₃@TiO₂ nanocomposites with enhanced dielectric properties and energy storage density. *Ceramics International*, 44(12), 13650-13656. <https://doi.org/10.1016/j.compositesa.2022.107019>
32. Xian, T., Yang, H., Di, L., Ma, J., Zhang, H., & Dai, J. (2014). Photocatalytic reduction synthesis of SrTiO₃-graphene nanocomposites and their enhanced photocatalytic activity. *Nanoscale Research Letters*, 9(1), 327. <https://link.springer.com/content/pdf/10.1186/1556-276X-9-327.pdf>
33. Kong, J., Rui, Z., & Ji, H. (2016). Enhanced Photocatalytic Mineralization of Gaseous Toluene over SrTiO₃ by Surface Hydroxylation. *Industrial & Engineering Chemistry Research*, 55(45), 11923-11930. <http://dx.doi.org/10.1021/acs.iecr.6b03270>
34. Li, D., Zeng, X., Li, Z., Shen, Z., Hao, H., Luo, W., Wang, X., Song, F., Wang, Z., & Li, Y. (2021). Progress and perspectives in dielectric energy storage ceramics. *Journal of Advanced Ceramics*, 10(4), 675-703. <https://doi.org/10.1007/s40145-021-0500-3>
35. Padurariu, L., Brunengo, E., Canu, G., Curecheriu, L. et al. V. (2023). Role of Microstructures in the Dielectric Properties of PVDF-Based Nanocomposites Containing -Permittivity Fillers for Energy Storage. *ACS Applied Materials & Interfaces*, 15(10), 13535-13544. . <https://doi.org/10.1021/acsami.2c23013>
36. Li, X., Yao, Z., Xie, J., Hao, et al. (2018). Grain boundary effects on piezoelectric properties of the core-shell-structured BaTiO₃@TiO₂ ceramics. *Journal of Advanced Dielectrics*, 8(06), 1850044. <https://doi.org/10.1142/S2010135X18500443>
37. Liu, X., Lv, S., Fan, B., Xing, A., & Jia, B. (2019). Ferroelectric Polarization-Enhanced Photocatalysis in BaTiO₃-TiO₂ Core-Shell Heterostructures. *Nanomaterials*, 9(8), 1116. <https://doi.org/10.3390/nano9081116>
38. Yuan, Y., Lin, J., Wang, X., Qian, J., Zuo, P., & Zhuang, Q. (2023). Achieving Excellent Dielectric and Energy Storage Performance in

- Core-Double-Shell-Structured Polyetherimide Nanocomposites. *Polymers*, 15(14), 3088. <https://doi.org/10.3390/polym15143088>
39. Zhou, J., Zhou, W., Yuan, M., et al. (2023). Significantly Suppressed Dielectric Loss and Enhanced Breakdown Strength in Core@Shell Structured Ni@TiO₂/PVDF Composites. *Nanomaterials*, 13(1), 211. <https://doi.org/10.3390/nano13010211>
40. Jesus, L. M., Barbosa, L. B., et al. (2023). Electrical microstructure evolution of CaCu₃Ti₄O₁₂ (CCTO) ceramics: From resistive and core shell-like to semiconducting grains. *Ceramics International*, 49(15), 25594-25601. <https://doi.org/10.1016/j.ceramint.2023.05.100>
41. Bouharras, F. E., Labardi, M., Tombari, E. et al. (2023). Dielectric Characterization of Core-Shell Structured Poly(vinylidene fluoride)-grafted-BaTiO₃ Nanocomposites. *Polymers*, 15(3), 595. <https://doi.org/10.3390/polym15030595>